Flexural Vibration Analysis of a Sandwich Beam Specimen with a Partially Inserted Viscoelastic Layer

Jin-Tack Park
Department of Mechanical Design and Production, Graduate School, Hanyang University, 17 Haengdang-Dong, Seongdong-ku, Seoul 133-791, Korea
Nak-Sam Choi*
Department of Mechanical Engineering, Hanyang University, 1271 Sa-1 dong, Ansan-si, Kyunggi-do 425-791, Korea

The flexural vibration characteristics of a sandwich beam system with a partially inserted viscoelastic layer were quantitatively studied using the finite element analysis in combination with the sine-sweep experiment. Asymmetric mode shapes of the flexural vibration were visualized by holographic interferometry, which agreed with those obtained by the finite element simulation. Effects of the length and the thickness of the partial viscoelastic layer on the system loss factor (η_s) and resonant frequency (f_r) were significantly large for both the symmetric and asymmetric modes of the beam system.

Key Words: Sandwich Beam Specimen, Viscoelastic Layer, Sine-Sweep Test, Flexural Vibration Damping, Resonant Frequency, Modal Strain Energy Method

1. Introduction

Recently, composite structures in the form of laminated construction composed of a constraining stiff layer and constrained viscoelastic layer have been applied in engineering designs for effective vibration damping and/or as a vibration absorber in mechanical systems. This is quite significant for better structural design since the vibration amplitude can be largely reduced during the resonance of the systems being subjected to dynamic loads.

For the elastic and viscoelastic layered sandwich beams with a finite length, Ditaranto (1965) proposed an auxiliary equation for analyzing the viscoelastic layer effects on the structural system loss factor. Trompette et al.(1978) studied a viscoelastically damped cantilever beam using finite element analysis and compared its results with experimental ones. Kim et al.(1992) analyzed the system loss factor of the sandwich beams considering the normal and shear deformation. For a partially covered sandwich beam, Lall et al.(1988) predicted the modal system loss factor by utilizing the Rayleigh-Ritz and Euler beam methods.

For a system consisting of a pair of parallel and identical elastic cantilevers which are lap-jointed by a viscoelastic layer, Saito and Tani (1984) derived theoretical equations for predicting the modal parameters such as the frequencies and loss factors of the coupled longitudinal and flexural vibrations as a function of the lap-joint length. Rao et al.(1990; 1992a: 1992b) proposed a theoretical model to evaluate the free flexural vibration of the bonded single-lap-joint beam and then described the effects of the thickness and modulus of the viscoelastic layer as well as the lap-joint length. Rao and He (1992c) also studied the modal damping ratio of a double-strap joint beam using finite element analysis. Johnson

* Corresponding Author,
E-mail: nschoi@hanyang.ac.kr
TEL: +82-031-400-5283; **FAX**: +82-031-406-5550
Department of Mechanical Engineering, Hanyang University, 1271 Sa-1 dong, Ansan-si, Kyunggi-do 426-791, Korea. (Manuscript **Received** December 26, 2002; **Revised** January 14, 2004)

and Kienholz (1992) proposed the modal strain energy method which may predict the loss factor of the structural system with a viscoelastic layer. Choi and Park (2001) proposed a theoretical analysis model for the flexural vibration of bonded single-lap-joint beams with the adhesion of partially covered sandwich-layer dampers.

This paper presents a finite-element analysis of the system loss factor and resonant frequency for a sandwich beam with a partially inserted viscoelastic layer. The sandwich beam system consists of a pair of parallel and identical cantilevers which are bonded on their free end parts by a viscoelastic film layer with a finite length. Resonant frequencies, mode shapes and loss factors of the system are measured using the sine-sweep test and the electronic speckle pattern interferometry, which are then compared with the results of the finite-element analysis. The effects of the length and thickness of the viscoelastic layer on the modal parameters for the asymmetric and the symmetric modes of the flexural vibration are investigated. This study focuses on the different behaviors of the modal parameters between the asymmetric modes showing the shear deformation in the viscoelastic layer and the symmetric modes showing the normal deformation, which should be related with some improvements in the system loss factor of such sandwich beams by geometrical variables.

2. Experimental Procedure

2.1 Specimen manufacturing

The cantilever beams for the sandwich beam systems in this study were made from unidirectional prepregs of carbon fiber/epoxy with a thickness of 125 μm (Cabonex, Hankook Fiber Co.). Two kinds of lay-ups were adopted using the prepregs: unidirectional 8 plies and 24 plies, which were cured in an autoclave according to the manufacturer's recommendations. The composite laminates so obtained had thicknesses of about 1 mm and 3 mm, respectively. They were sectioned utilizing a diamond wheel cutter to make the composite cantilever beams with a width of 5 mm and a length of 200 mm.

Sandwich beam specimens were manufactured by inserting a viscoelastic adhesive film (Scotch Damp ISD 112 damping film, 3M Corp.) with a length of l_v between two composite beams, as illustrated in Fig. 1. The storage shear modulus and the material loss factor η_d (=tan δ) of the film at the temperature of 20℃ are presented in Fig. 2. In a frequency range of 10 to 1200 Hz, the loss factor is a constant of about 0.9, and the storage shear modulus increases almost linearly with increasing frequency. The thicknesses of the viscoelastic films were selected to be 50, 250 and 500 μm with lengths of 10, 30, 60, 120 and 150 mm, respectively. Aluminum foils with the same thickness as the viscoelastic films were inserted up to 50 mm into the left end part between the cantilever beams in order to keep two cantilever beams parallel, and thus, to remove any frictional contacts during the vibration test. Thus, the sandwich beam specimens formed a symmetric lay-up geometry with an effective length (L) of 150 mm.

The sandwich beam specimens were put on a steel plate and covered with a breather and a

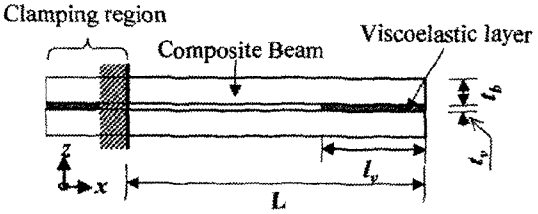

Fig. 1 Sandwich beam specimen adhered with a partially inserted viscoelastic layer

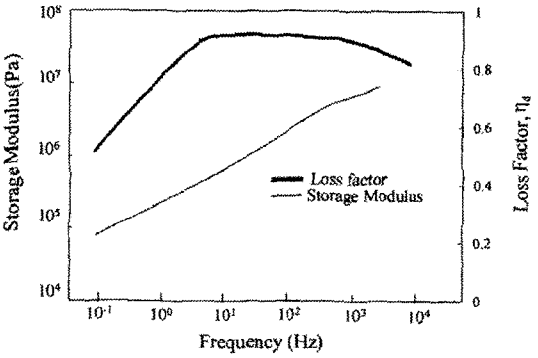

Fig. 2 Storage modulus and loss factor of the viscoelastic layer material

vacuum bagging film. Sealants were adhered between the bagging film and a steel plate. The specimens were then maintained at 20℃ in a vacuum state so that voids could be removed in the viscoelastic adhesive layer between two beams. A pressure of 3 atm pressure was maintained for 1 hour in an autoclave to form a perfect bonding between the beams. After finishing the bonding process, the pressure state of the specimens was relieved to the atmospheric pressure.

2.2 Sine sweep test

The sandwich beam specimen was mechanically fixed by a clamping device which had been installed on a vibration exciter (model 4808, B& K Co.). A sine sweep test was carried out by exciting the clamping device to induce a lateral vibration of the effective length part of the specimen in a frequency range of 1 to 1200 Hz. A non-contact laser sensor detected the dynamic displacement of the specimen surface at a location 5 mm distant from the free end of the sandwich beam. A frequency response function (FRF) curve was measured through a dynamic signal analyzer (HP 35670A). The modal frequency f_r (i.e., resonant frequency at the r-th mode) was measured corresponding to the r-th peak value in the FRF curve. The structural system loss factor ($\eta_s^{(r)}$) at the r-th mode was obtained using the half power bandwidth method (Paz 1997, i.e., through Equation (1) based on the frequencies (f_1, f_2) corresponding to the value of magnitude 3dB less than the r-th peak value in the FRF curve).

$$\eta_s^{(r)}=\frac{2(f_2-f_1)}{f_1+f_2} \tag{1}$$

2.3 Visualization of mode shapes by a stroboscopic ESPI

Stroboscopic electronic speckle pattern interferometry (three dimensional ESPI system, Ettemeyer Co.) was used for visualizing the resonant mode shapes of the sandwich beam specimens. This experiment was performed on a vibration-free table for a good ESPI measurement. First, the speckle image of an undeformed specimen was taken. Next, the effective length part of the specimen was vibrated laterally by excitation of the clamping device through a thin steel wire. The wire was connected longitudinally to the axis of the vibration exciter which had been isolated from the working table. The exciting frequency was chosen to be the resonant frequency at each mode which had been measured by the above sine sweep test. During the excitation, an acoustic optical modulator was synchronized with the exciting frequency. The synchronized laser pulse was projected onto the specimen to generate the stroboscopic effect, so that a constant image of the resonant specimen could be formed. The digitized speckle images of undeformed and deformed (vibratory) configurations of the specimen were correlated to form interferometric fringes. Thus, deformation mode shapes for the transverse vibration of the sandwich beam specimen was visualized through an ESPI analysis software.

3. Finite Element Analysis

A two dimensional finite element approach to model the sandwich beam system in Fig. 1 was performed using the commercial software Ansys ver. 5.3 for comparison with the above experiment. A finite-element model mesh exhibited in Fig. 3 was adopted to calculate the strain energy distribution in the deformed beam system. The sandwich beam model had a constant width in the y-direction and was fixed at the left end. The length (l_v) and thickness (t_v) of the viscoelastic layer as well as the thickness (t_b) of the beam were treated as variables. The effective length (L) of the cantilever beams was assumed to be constant (150 mm).

The model was made up of two-dimensional isoparametric plane strain rectangular elements (Plane42) with 4 nodes. Each node had two

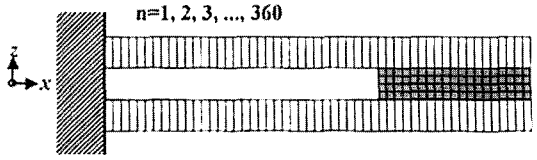

Fig. 3 Finite element modeling

degrees of freedom, u and v. Each beam had 360 elements in the lengthwise direction (x-direction) and 1 element in the thickness direction (z-direction), and the viscoelastic layer had 4 elements in the thickness direction (z-direction). The respective elements in the elastic beam and the viscoelastic layer were kept to 150/360 mm in length (x-direction). Thus, the total number of elements in each beam was 360, while that of the viscoelastic layer varied with the length of l_v. For example, the number of elements in the viscoelastic layer was 96 ($=24\times4$) for $l_v=10$ mm and 1440 ($=360\times4$) for $l_v=150$ mm. There was a perfect continuity at the interfaces between the beam and the layer and no slip arose along the interface. Elastic modulus of the composite beam was selected according to the static bending test results (E=104.83 GPa and 72.92 GPa for $t_b=1$ and 3 mm, respectively). Its density was 1479.2 kg/m^3. Elastic modulus and material loss factor of the viscoelastic layer were chosen from the data curves in Fig. 2 (offered by 3M Co.) in accordance with the experimentally measured resonant frequency of the sandwich beam specimen at each vibration mode. Poisson's ratio of the viscoelastic layer was assumed to be 0.45.

Based on the modal analysis for the free flexural vibration of the beam specimen, the modal frequencies (resonant frequencies at the respective modes) and mode shapes were obtained. The system loss factor at each mode r was evaluated through the modal strain energy method (Johnson and Kienholz, 1992; Choi and Park, 2001) which is based on the principle that the ratio of the composite system loss factor $\eta_s^{(r)}$ to the viscoelastic material loss factor $\eta_d^{(r)}$ for a given vibration mode (r) can be estimated as the ratio of the elastic strain energy stored in the viscoelastic material U_{visco} to the total elastic strain energy stored in the entire structure U_{total} when it deforms in an undamped mode shape:

$$\frac{\eta_s^{(r)}}{\eta_d^{(r)}}=\frac{\{\phi^{*(r)}\}^T[K_{vR}]\{\phi^{*(r)}\}}{\{\phi^{*(r)}\}^T[K_R]\{\phi^{*(r)}\}}=\frac{U_{\text{visco}}}{U_{\text{total}}} \quad (2)$$

where $[K_{vR}]$ is the real part of the stiffness matrix for the viscoelastic layer; $[K_R]$ the real part of the stiffness matrix for the total structure; and $\{\phi^{*(r)}\}$ the eigenvector at the r-th mode. Without consideration of the damping loss in the viscoelastic layer, the eigenvalue problem for the finite element model was solved in ANSYS version 5.3 (Kohnke, 1995). The modal analysis offers not only the modal frequencies but also the corresponding modal strain energies U_{visco} and U_{total}, with which $\eta_s^{(r)}$ can be estimated through Equation (2) at a given value of $\eta_d^{(r)}$.

4. Results and Discussion

4.1 Experimental frequency responses

Figure 4 shows the frequency response curves measured by the sine sweep test for a single beam specimen (1 mm in thickness and 150 mm in effective length) and two kinds of sandwich beam specimens with a partially-inserted viscoelastic layer ($l_v=10$ mm) and with a fully-inserted one ($l_v=150$ mm). The beam thickness (t_b) for the sandwich specimens was kept to 1 mm. The frequencies for the 1st and 2nd modes could be determined at the corresponding resonant peaks in the curve. The sharpness and magnitude level of each peak were progressively degraded, and resonant frequency at each mode had a tendency to increase in the order of single beam, sandwich beam with $l_v=10$ mm and sandwich beam with $l_v=150$ mm. This indicates that the system damping as well as the stiffness of the sandwich specimen increased considerably with an increase in the length of the viscoelastic layer. Other peaks corresponding to the 3rd and higher modes were

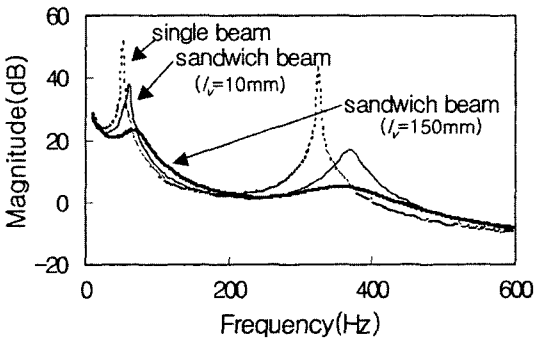

Fig. 4 Experimental frequency response of a single beam and sandwich-bonded beams ($t_b=1$ mm, $t_v=500$ μm)

not observable for the current sandwich beam specimens. Similar features of system damping and stiffness effects were also observed for $t_b=3$ mm.

4.2 Visualization of mode shapes of the flexural vibration

On the basis of the resonant frequencies measured with the sine sweep test, actual mode shapes of a sandwich beam specimen with $l_v=10$ mm, $t_b=1$ mm and $t_v=500$ μm for the 1st and 2nd modes were visualized using a stroboscopic ESPI apparatus. The mode shapes are shown in Fig. 5(a) and (b), respectively. Fig. 6(a) and (b) exhibits results of the 1st and 2nd mode shapes calculated by finite-element analysis with the geometrical and material conditions similar to the above sandwich specimen. The visualized images were in a form of asymmetric modes, which were comparable for both ESPI experiment and finite-element simulation. This may indicate that resonant frequency and system loss factor can be reasonably evaluated through comparison between the sine sweep test and finite element analysis. It is to be noted that the asymmetric mode shapes of the sandwich beam follows the basic shapes corresponding to the 1st and 2nd modes of a single beam. Since for the asymmetric modes of vibration of the sandwich beam specimen the bottom surface of the upper beam deforms out-of-phase with the top surface of the lower beam, the viscoelastic layer adhered between the beams suffers a shear deformation. The effect of viscoelastic layer on the modal parameters may be distinguished through the experimental test and the finite element simulation: Experimental results measured by the ESPI system (see Fig. 5) show that the amplitude level at the 2nd mode was about 1/13 times lower than that at the 1st mode, which agreed well with the results by the sine sweep test (see Fig. 4) in that the magnitude at the 2nd mode was lower by 23dB than that at the 1st mode. The amplitude level for the higher modes became much lower and was below the noise level of measurement.

Although the mode shape for the 3rd mode was unmeasurable under the present experimental condition, a finite element analysis offered a symmetric mode shape for the 3rd mode, as shown

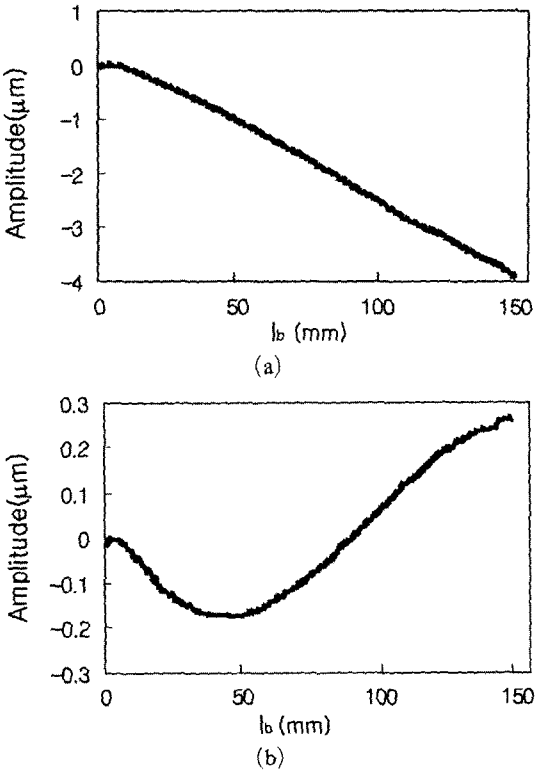

Fig. 5 Mode shapes of a sandwich beam with a partially inserted viscoelastic layer ($t_b=1$ mm, $t_v=500$ μm, $l_v=10$ mm) visualized by the stroboscopic ESPI: (a) 1st mode (b) 2nd mode

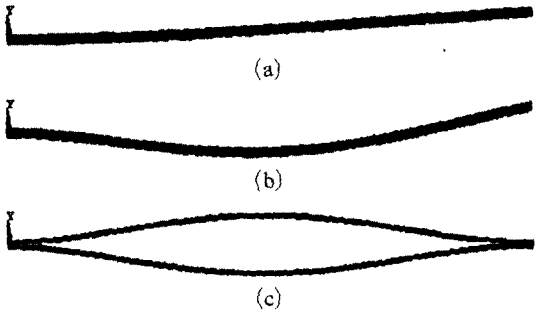

Fig. 6 Mode shapes of a sandwich beam with a partially inserted viscoelastic layer ($t_b=1$ mm, $t_v=500$ μm, $l_v=10$ mm) visualized by FE simulation: (a) 1st (anti-symmetric), (b) 2nd (anti-symmetric) and (c) 3rd (symmetric) modes

in Fig. 6(c). Because, for the symmetric mode, the bottom surface of the upper beam deforms a in-phase with the upper surface of the lower beam, a normal (tensile/compressive) deformation occurred in the viscoelastic layer between the beams. However the shape of each beam did not follow any mode shapes of a single beam. This may induce vibration with characteristics different from that of the asymmetric mode.

4.3 Resonant frequency and loss factor of sandwich beam specimens

As mentioned above, the sandwich beam systems with a partially-inserted viscoelastic layer generated asymmetric and symmetric mode shapes during their flexural vibrations. Resonant frequency and loss factor of the beam system at each mode are evaluated in the following as a function of the thickness and the length of the viscoelastic layer. For the 1st and the 2nd modes corresponding to the asymmetric mode shapes, the vibration behaviors are described by finite element analysis (FEA) and then compared with those obtained by a sine-sweep test. For the 3rd mode with a symmetric mode shape, the vibration behaviors are evaluated only through finite element analysis.

4.3.1 Asymmetric mode

Figure 7 shows resonant frequency (f_r) of the sandwich beam systems with a fully-inserted viscoelastic layer (l_v=150 mm) as a function of the thickness of the viscoelastic layer (t_v). Solid and dotted lines in the figure represent results for beam thicknesses (t_b) of 1 mm and 3 mm, respectively. Experimental values agreed well with those obtained by the FEA. Resonant frequency for each mode decreased with an increase of t_v. This is understandable in that first, f_r at each mode can be described through the equivalent spring-mass resonance equation (Paz, 1997)

$$f_r=\frac{1}{2\pi}\cdot\left(\frac{K_e}{M}\right)^{1/2} \tag{3}$$

where M and K_e are the total mass and the effective flexural stiffness of a sandwich beam specimen, respectively; and second, an increase of t_v caused a considerable decrease in shear stiffness as well as an increase in weight of the viscoelastic layer bonded between the upper and lower beams. Resonant frequencies for the respective modes in case of t_b=3 mm were much higher than the corresponding frequencies for t_b=1 mm, which is reasonable on Equation (2) in consideration of the fact that an increase of the beam thickness enlarges the effective flexural stiffness of the sandwich beam system according to a simple beam theory.

Figure 8 shows behaviors of f_r for the sandwich beam systems with t_v=500 μm as a function of the length of the viscoelastic layer (l_v). Results obtained for t_b=1 mm by the FEA and the sine-sweep test agreed well with each other. For the 1st mode, f_r showed a gradual increase

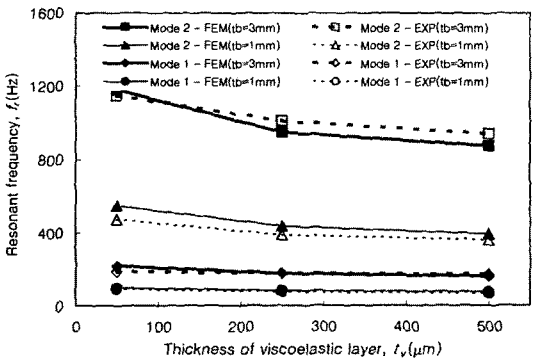

Fig. 7 Resonant frequency of the sandwich beam system as a function of the thickness of the viscoelatic layey (l_v=150 mm)

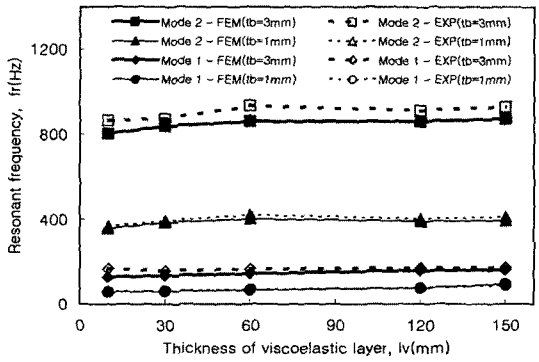

Fig. 8 Resonant frequency of the sandwich beam system as a function of the length of the viscoelatic layer (t_v=500 μm)

with increasing l_v. This is because an increase of l_v reduced the vacant space in the intermediate layer between the upper and lower beams, and thus made the stiffness of the beam system greater. For the 2nd mode, f_r increased with an increase of l_v from 10 mm to 60 mm ; however, it revealed a nearly constant value in the range of l_v beyond 60 mm. It is thought that the increase of l_v induced some increases in weight of the system which might suppress the increase of f_r on the basis of Equation (2). Behaviors of the variation of f_r with l_v for $t_b=3$ mm were very similar to those for $t_b=1$ mm stated above.

Figure 9 shows system loss factor $\eta_s^{(r)}$ of the sandwich beam specimens with $l_v=150$ mm as a function of t_v. For $t_b=1$mm, the value of $\eta_s^{(r)}$ at $t_v=50$ μm for the 1st mode was lower than that for the 2nd mode. However in the range $t_v \geq 250$ μm, $\eta_s^{(r)}$ for the 1st mode was higher since it increased drastically with an increase of t_v as compared with the behavior for the 2nd mode. Although values of $\eta_s^{(r)}$ calculated by the FEA showed some amount of underestimation in comparison with those measured by the sine-sweep test (this may be caused by analytical and experimental errors.), the variation tendency of $\eta_s^{(r)}$ with t_v agreed with each other. Considering that loss factor of the viscoelastic layer ($\eta_d^{(r)}$) was a constant of about 0.9 in a range of resonant frequencies shown in Fig. 7, the above variation of $\eta_s^{(r)}$ was dependent on the ratio of the strain energy stored in the viscoelastic layer U_{visco} to the strain energy stored in the total system U_{total} as supposed in Equation (2). Therefore it is to be mentioned that these kinds of composite structures may show a characteristic of low system loss factor at high resonant frequency, which depends on t_v, and thus, on the amount of U_{visco}/U_{total}.

On the other hand, a similar feature of the variation in $\eta_s^{(r)}$ was also observed for $t_b=3$ mm. Values of $\eta_s^{(r)}$ were 0.18~0.28, which were considerably low, and thus, slightly dependent on the vibration modes and amounts of t_v in comparison with those for $t_b=1$ mm. This may be understood on the basis of Equation (2) in that the stiffness matrix of the beam system $[K_R]$ increases significantly for $t_b=3$ mm while $[K_{vR}]$ of the viscoelastic layer exhibits only a small change.

Figure 10 shows behaviors of $\eta_s^{(r)}$ as a function of l_v for the sandwich beam specimens with $t_v=500$ μm. It is obvious according to Equation (2) that first, $\eta_s^{(r)}=0$ at no amount of viscoelastic layer ($l_v=0$) ; and second, an increase of l_v brings about an increase of U_{visco}, and thus, an increase in $\eta_s^{(r)}$ for the respective modes. In this figure experimental results agreed well with those obtained by the FEA. The increasing slope of $\eta_s^{(r)}$ was the steepest in the initial stage of l_v from 0 to 10 mm. After that, $\eta_s^{(r)}$ increased with a lessened slope. Values of $\eta_s^{(r)}$ for the 1st mode were larger than those for the 2nd mode, and values for $t_b=3$ mm were much lower than those for $t_b=1$ mm, which was consistent regardless of

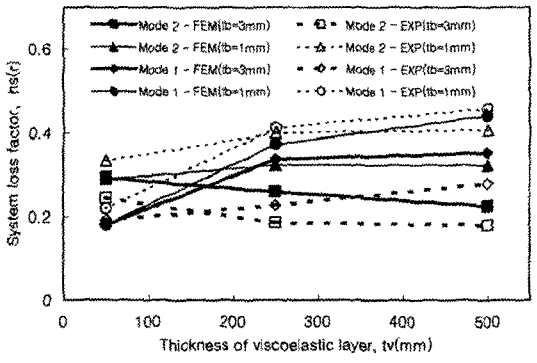

Fig. 9 System loss factor of the sandwich beam specimens as a function of the thickness of the viscoelastic layer ($l_v=150$ mm)

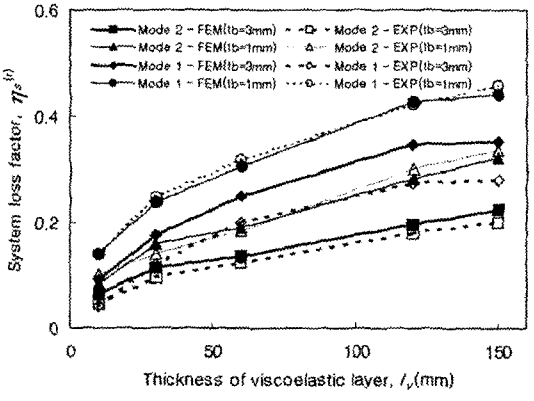

Fig. 10 System loss factor of the sandwich beam specimens as a function of the length of the viscoelastic layer ($l_v=500$ μm)

the amount of l_v.

4.3.2 Symmetric mode

Although the behavior of vibration for the symmetric mode of the sandwich beam system was hardly detectable under the present experimental conditions, it was definitely existent as a result of FEA, shown in Fig. 6(c). Under geometric conditions of the beam thickness $t_b=1$ mm and the short viscoelastic layer with $l_v \leq 60$ mm and $t_v \geq 250$ μm, the 1st symmetric mode could appear as the 3rd mode (see Fig. 6(c)) which had a higher resonant frequency than the above asymmetric modes. Considering that resonant mode arises when the mechanical impedance (i.e., the ratio of force to deformation velocity) becomes minimal, the symmetric mode of vibration in a low frequency range must have had a higher mechanical impedance than the asymmetric mode. Since the above experimental results for the asymmetric modes agreed considerably with the FEA results, it is thought that the resonant frequency and loss factor for the symmetric mode of the beam systems evaluated only by the FEA are quite reasonable.

Because the experimental values of the resonant frequency for the symmetric mode were barely obtained, the elastic modulus of the viscoelastic layer corresponding to the experimental resonant frequency for the 2nd anti-symmetric mode was first selected in the data curve in Fig. 2. The selected value was input as an elastic modulus of the viscoelastic layer in the finite-element model, and then, resonant frequency at the 1st symmetric mode (mainly the 3rd mode among the entire modes) was numerically obtained. Values of elastic modulus and material loss factor of the viscoelastic layer corresponding to the numerically obtained frequency were selected again in Fig. 2, with which accurate resonant frequency and system loss factor for the 1st symmetric mode could be evaluated.

Figure 11 shows behaviors of resonant frequency for the 1st symmetric mode of the sandwich beam specimens with $t_b=1$ mm as a function of l_v. The behavior of resonant frequencies obtained at $t_v=500$ μm was scarcely different from that at $t_v=250$ μm. f_r increased gradually with an increase of l_v to 60 mm; however, it drastically increased around $l_v=120$ mm to a value about 7.8 times larger than that at 60 mm. At this value of $l_v=120$ mm, the asymmetric modes were formed until the 7th mode, and thus the 1st symmetric mode corresponded to the 8th mode among the entire modes. This indicates that it was difficult to form the low-order symmetric mode because of high mechanical impedance as l_v became large. The symmetric mode of the sandwich specimen in a state of full insertion ($l_v=150$ mm) did not arise in the present frequency range. Moreover, the symmetric mode was not observed at any l_v values for $t_b=3$ mm. This represents that the mechanical impedance for the symmetric mode increased greatly as t_b became thick. It is thought that thin beams as well as a short and thick viscoelastic layer are required to obtain the low-order symmetric mode.

Figure 12 shows behaviors of $\eta_s^{(r)}$ for the 1st symmetric mode obtained as a function of l_v under the analytic conditions of Fig. 11. $\eta_s^{(r)}$ was

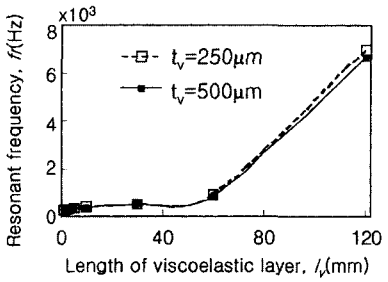

Fig. 11 Resonant frequency of the sandwich beam specimens as a function of the length of viscoelastic layer

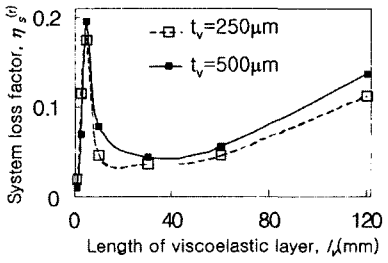

Fig. 12 System loss factor of the sandwich beam specimens as a function of the length of the viscoelastic layer

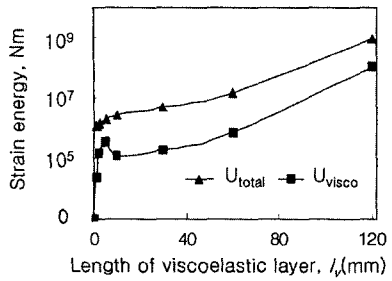

Fig. 13 Strain energy of the sandwich beam system and the viscoelastic layer (t_v=250 μm)

zero at l_v=0. $\eta_s^{(r)}$ drastically increased in the initial stage of l_v and reached the maximum value around l_v=5 mm. With an increase of l_v to 10 mm, it rapidly decreased and was minimized around l_v=30 mm. After that, $\eta_s^{(r)}$ showed a gradual increase with increasing l_v. The characteristic behavior of $\eta_s^{(r)}$ for the 1st symmetric mode had a tendency similar to the theoretical results suggested by Saito and Tani (1984). Based on equation (2), $\eta_s^{(r)}$ depends on U_{visco}/U_{total}. As compared with U_{total}, U_{visco} for the 1st mode exhibited a feature (see Fig. 13) similar to the above behavior of $\eta_s^{(r)}$: a drastic increase in the initial stage of l_v, a peak around l_v=5 mm, and after that, a rapid decrease and then a gradual increase with increasing l_v. It is thought that the above feature of $\eta_s^{(r)}$ was primarily affected by such behavior of U_{visco} which was produced due to some differences in the shape and size of deformation of the viscoelastic layer in the sandwich beam portion changing with the amount of l_v. On the other hand, values of $\eta_s^{(r)}$ at t_v= 500 μm were slightly larger than those at 250 μm. The variation behavior of $\eta_s^{(r)}$ with l_v scarcely depended on the amount of t_v.

5. Conclusions

Resonant frequency and loss factor of a sandwich beam system with a partially inserted viscoelastic layer have been evaluated as a function of the length and the thickness of the viscoelastic layer as well as the beam thickness.

(1) Variations of resonant frequency f_r and loss factor $\eta_s^{(r)}$ of the system obtained by the finite-element analysis agreed well with those obtained by the sine-sweep test.

(2) For the asymmetric mode, system loss factor $\eta_s^{(r)}$ of the sandwich beam specimen having thin beams was larger than that of the specimen having thick beams. $\eta_s^{(r)}$ increased with an increase in the length of the viscoelastic layer. As the thickness of the viscoelastic layer increased to and beyond 250 μm, $\eta_s^{(r)}$ for the 1st mode became larger than that for the 2nd mode.

(3) For the symmetric mode confirmed by the finite-element analysis, $\eta_s^{(r)}$ showed a large variation with the length of the viscoelastic layer: a drastic increase in the initial stage of l_v, and then, formation of a peak. With further increase of l_v, a decrease and, after that, a gradual increase. The variation of $\eta_s^{(r)}$ was hardly dependent on the thickness of the viscoelastic layer. The systems with thick beams did not form a symmetric mode shape.

(4) It is expected that the above results can be used for better understanding of effective vibration damping of composite structures with constrained viscoelastic layers.

References

Choi, N. S. and Park, J. I., 2001, "Analysis of the Vibration Damping of Bonded Beams with a Single-Lap-Joint and Partial Dampers," *JSME International Journal Series C*, Vol. 44, No. 2, pp. 350~359.

Ditaranto, R. A., 1965, "Theory of Vibratory Bending for Elastic and Viscoelastic Layered Finite-Length Beams," *Journal of Applied Mechanics*, Vol. 32, pp. 881~886.

Johnson, C. D. and Kienholz, 1992, "Finite Element Prediction of Damping in Structures with Constrained Viscoelastic Layers," *D.A., AIAA Journal*, Vol. 20, pp. 1284~1290.

Kim, C. H. and Park T. H., 1992, "Analytical and Experimental Study on the Damping of Vibrating Layered Plates Including the Effects of Shear and Thickness Deformation of the Adhesive Layer," *Journal of the Korean Society of Mechanical Engineers*, Vol. 7, pp. 1224~1254.

Kohnke, P., 1995, *Ansys Manual : Theory*

Reference-Release 5.3, Ansys Inc., Houston.

Lall, A. K., Asnani, N. T. and Nakra, B. C., 1988, "Damping Analysis of Partially Covered Sandwich Beams," *Journal of Sound and Vibration*, Vol. 123(2), pp. 247~259.

Paz, M., 1997, *Structural Dynamics : Theory and Computation*, Chapman & Hall, New York.

Rao, M. D. and Crocker, M. J., 1990, "Analytical and Experimental Study of the Vibration of Bonded Beams with a Lap Joint," *Trans. of the ASME, J. of Vibration and Acoustics*, Vol. 112, pp. 444~451.

Rao, M. D. and He, S., 1992a, "Vibration Analysis of Adhesively Bonded Lap Joint, Part I : Theory," *Journal of Sound and Vibration*, Vol. 152(3), pp. 405~416.

Rao, M. D. and He, S., 1992b, "Vibration Analysis of Adhesively Bonded Lap Joint, Part II : Numerical Solution," *Journal of Sound and Vibration*, Vol. 152(3), pp. 417~425.

Rao, M. D. and He, S., 1992c, "Analysis of Natural Frequencies and Modal Loss Factors of Simply Supported Beams with Adhesively Bonded Double-Strap Joints," *Journal of Acoustical Society of America*, Vol. 92(1), pp. 268~276.

Saito, H. and Tani, H., 1984, "Vibrations of Bonded Beams with a Single Lap Adhesive Joint," *Journal of Sound and Vibration*, Vol. 92 (2), pp. 299~309.

Trompette, P., Boillot, D. and Ravanel, M. A., 1978, "The Effect of Boundary Conditions on the Vibration of a Viscoelastically Damped Cantilever Beam," *Journal of Sound and Vibration*, Vol. 60(3), pp. 345~350.